Comparison between AGC and a Tuning-less LFC Approach Based on Direct Observation of DERs

Prostejovsky, Alexander Maria; Marinelli, Mattia

Published in:
Proceedings of the 52nd International Universities' Power Engineering Conference

Publication date:
2017

Document Version
Peer reviewed version

Comparison Between AGC and a Tuning-less LFC Approach Based on Direct Observation of DERs

Alexander M. Prostejovsky and Mattia Marinelli
Center for Electric Power and Energy, Department of Electrical Engineering,
DTU – Technical University of Denmark, Roskilde, Denmark.
Email: {alepros,matm}@elektro.dtu.dk

***Abstract*—Automatic Generation Control (AGC) used in secondary frequency control requires manual tuning to maintain a balance between reaction speed and stability. This task becomes increasingly difficult due to the rising number of inverter-coupled devices and High-Voltage Direct Current (HVDC) links, and the resulting reduction of available inertia. In this paper, we propose a tuning-less Load-Frequency Control (LFC) approach able to cope with the changing dynamics of electric power grids. Harnessing the possibilities of modern monitoring and communication means, the so-called Direct Load-Frequency Control (DLFC) employs two concurrently operating processes: a power matching stage responsible for secondary power adjustment using directly observed area imbalances; and a frequency control stage that adjusts primary reserves' frequency setpoints in a systematic manner. As opposed to the AGC, the DLFC does not require an integrator to mitigate frequency deviations. The only free parameter is the secondary control interval, from which all other parameters are derived. Small-signal stability investigations show that the DLFC exhibits 40 dB falloff of steady-state deviations versus the AGC's 20 dB. Simulations on the non-linear single-area system confirm the DLFC's response speed and stability advantage.**

***Index Terms*—Automatic Generation Control, Distributed Systems, Load Frequency Control, Low Inertia Systems, Power Quality, Renewable Energy Sources**

I. Introduction

The electric power grid faces significant changes due to its increasing penetration with renewable energy sources. Bulk generators, comprised of rotating machines that contribute to grid stability with inertia, are gradually replaced by inverter-coupled devices in the low- and medium-voltage levels [1]. The expansion of High-Voltage Direct Current (HVDC) infrastructure decouples the inertial response between control areas even further, making the grid more susceptible to transient events [2]. Planning uncertainty due to the high volatility of Renewable Energy Source (RES) (e.g., wind and solar power) contributes to stability problems [3]. Currently employed Automatic Generation Control (AGC) uses PI-controllers to obtain the secondary regulation signals [4]. Tuning of the corresponding controller parameters is performed manually under consideration of the various generator non-linearities. The resulting controller is rigid, and its performance is slow in order to keep the stability margin high. Consequently, we see a rising number of frequency incidents, as for example reported by the European Network of Transmission System Operators for Electricity (ENTSO-E) for the Nordic Grid [5].

Alternative Load-Frequency Control (LFC) concepts for interconnected power systems have been proposed, focusing mainly on adaptive tuning and Multi-objective Optimization Problems (MOPs). Adaptive approaches aim for automatic tuning of the AGC's PI-controller with minimal model knowledge. Optimization-based controllers are for example proposed in [6], [7], whereas machine learning is employed in [8], [9]. MOP approaches derive optimal setpoints based on representative physical models augmented with the observed system state. A centralized Model Predictive Control (MPC) take on MOP applicable to smaller synchronous areas is presented in [10]. Distributed Model Predictive Control (DMPC) decomposes the MPC problem into several smaller ones and involves active data exchange between the individual controllers, as demonstrated in [11], [12], [13]. Extensive in-depth surveys on alternative LFC control strategies are covered in [14]. Most approaches, however, suffer from drawbacks concerning their implementability. Adaptive controllers' stability is hard to prove and subject of ongoing research [15], and MOP-based controllers are virtually infeasible in presence of the rising complexity of modern grids.

With the rapid expansion of monitoring infrastructure in distribution grids [16], [17], and the increasingly active role of Distribution System Operators (DSOs) in grid management [18], new solutions to LFC become possible. The DSOs' awareness of available flexibility through monitoring infrastructure close to customers and DERs [19], [20] can be harnessed for real-time control [21], [22]. Information and Communication Technology (ICT) is regarded as the key enabling factor [23] for Smart Grids (SGs), for which reason standardized data exchange policies and Transmission System Operator (TSO)-DSO data interfaces are established [24], [25]. Therefore, it is reasonable to assume that near-complete observability of the electric grid will be achieved in the foreseeable future.

This work presents a novel tuning-free LFC approach called Direct Load-Frequency Control (DLFC). The DLFC makes use of the aforementioned modern means of monitoring and communications to directly observe area imbalances, allowing for fast determination of secondary power setpoints. In addition, primary devices are actively involved in frequency control by remotely adjusting their reference frequency setpoints. By inferring the frequency over the primary resources' power output and their droop, frequency is treated as a local

quantity. Frequency control is therefore effectively decoupled from system non-linearities and does not require integrators to mitigate steady-state errors, and secondary power is only activated in response to load events but not frequency deviations. While we assume a high degree of state awareness, frequency control works also under partial observability. The DLFC' performance is investigated in two different simulation scenarios and compared against the AGC, against which it shows stability and speed advantages without the respective tuning effort. Compared to MOP approaches which generally rely on high observability as well, the requirements on the power systems model are the same as for the AGC.

The work is structured as follows. Section II introduces the AGC in detail and gives an overview on the proposed DLFC approach. Section III contains the considered power systems model and the proposed DLFC methodology. Section IV describes the simulation scenarios used for the small-signal stability analysis and a transient response comparison of AGC and DLFC. Finally, Section V concludes the simulation results and addresses open issues and potential future works.

II. Comparison between AGC and DLFC

This section introduces the AGC in detail and provides a comparison to the proposed DLFC approach.

A. Automatic Generation Control

AGC is the most common realization of LFC. Its input signal is the Area Control Error (ACE) $P^{\text{ACE}} = \Delta P^{\text{tie}} + B\Delta f$, where $\Delta P^{\text{tie}} = P^{\text{tie}} - P^{\text{tie}}_{\text{sched}}$ is the deviation of the combined tie-line flows P^{tie} from their scheduled values $P^{\text{tie}}_{\text{sched}}$, and B is the bias factor [4]. The bias factor represents the area's frequency response characteristic, consisting of primary devices' speed droop k and the load-damping constant D of frequency dependent loads. Secondary power setpoints are determined by the AGC's PI-controller

$$P^{\text{sec}} = V^P P^{\text{ACE}} + \frac{1}{T^I}\int_{t_0}^{t} P^{\text{ACE}}(\tau)\, d\tau \tag{1}$$

using the proportional gain V^P and the integral time constant T^I. These parameters are chosen based on observations of the area response following major grid events (e.g., loss of bulk generators), and are further adjusted during normal operation. The resulting secondary power is subsequently shared across units participating in secondary control. Fig. 1 shows the corresponding signal flows in the left half.

B. Proposed DLFC Approach

The proposed approach differs from the traditional AGC approach in the required live situational awareness. Where the AGC is based on tie-line and frequency measurements to infer the area imbalance, we assume a high degree of direct observability of the area's internal state using modern ICT and monitoring as described in Section I. The term *cell* is used in place of of *area* to highlight the differences. We make the following assumption on cells:

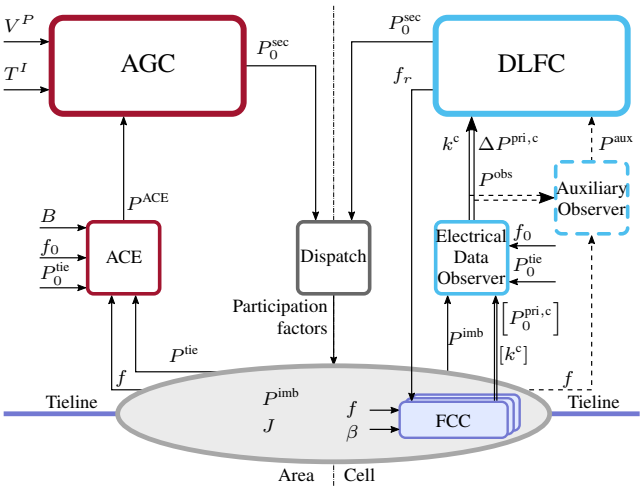

Fig. 1. Structural overview of AGC versus DLFC signal flows.

- They exhibit a high degree of internal observability through direct measurements, lumped states from aggregators, and state estimators, which are all represented in a so-called Electrical Data Observer (EDO), which is not part of the study;
- Remotely adjusting the reference frequencies of primary resources participating in DLFC is possible;
- The droop of participating primary resources is known.

More information on cells and the related Web-of-Cells (WoC) concept for interconnected power system is available in [26] and [27].

The signal flows of the DLFC are shown in the left half of Fig. 1. State information from the cell is gathered by the EDO, which feeds the DLFC as well as the optional auxiliary observer. Primary resources actively participating in control supply, denoted as Frequency Containment Control (FCC), supply the EDO with their current nominal setpoints and droop gains (assumed to be variable in the WoC context) and receive frequency reference setpoints by the DLFC. Secondary power setpoints of the DLFC are processed by a dispatcher just as in the AGC. The DLFC's mathematical description is presented in the following.

III. Methodology

The derivation of the DLFC's mathematical description as well as the underlying cell model is based on the definitions in Section II. We assume a generation-oriented frame of reference (power flows into cells are positive).

A. Cell Model

The swing equation

$$J\omega\dot{\omega} = P^{\text{imb}} \tag{2}$$

represents the dynamic behavior of the considered control area, with J as the total inertia, $\omega = 2\pi f$ as the (angular) frequency, and the area imbalance P^{imb} [4]. We define the latter as

$$P^{\text{imb}} = P^{\text{pri}} + P^{\text{sec}} + P^{\text{uc}} + P^{\text{uo}} \tag{3}$$

with the contributions of primary and secondary resources P^{pri} and P^{sec}, the observed but uncontrolled load and generation P^{uc}, and the total unobserved power P^{uo} (e.g., unmeasured consumption, unaccounted losses). Primary resources follow the droop control law

$$P^{\text{pri}} = P_0^{\text{pri}} - k\,(f - f_r)\,, \tag{4}$$

where P_0^{pri} is the base generation at f_0, k the droop gain, and f_r the reference frequency typically chosen as f_0 (e.g., $50\,\text{Hz}$ in Europe). We assume that the operating state of all controlled primary and secondary resources can be observed in real-time, and that the droop gain of primary resources is known.

B. Secondary Control

Secondary control performed by the DLFC is a twofold process executed in $T_{\text{c}}^{\text{sec}}$ intervals. Each timestep $t = nT_{\text{c}}^{\text{sec}}$ is indexed by the variable n. The control signals are subsequently low-pass filtered and sent to the distributed controller.

1) Power Balancing: The AGC senses area imbalances over the ACE as described in Section II-A and needs to be tuned both against the estimated area bias and the non-linearities of the controlled resources. On the other hand, the DLFC uses direct observations of the area's production and consumption to infer the optimal secondary power setpoint.

By letting $P^{\text{sec}} = 0$ and $P^{\text{uo}} = 0$ in (3), the observed imbalance in the area is

$$P^{\text{obs}}(n) = P_0^{\text{pri}}(n) + P^{\text{uc}}(n). \tag{5}$$

Here, the nominal primary setpoint P_0^{pri} is used in place of the actual value P^{pri} in order to free the primary reserves at f_0 and avoid mutual coupling effects.

Assuming a high degree of observability and therefore a good knowledge of imbalances, secondary reserves can be directly set to

$$P^{\text{sec},*}(n+1) = -P^{\text{obs}}(n) + P^{\text{aux}}(n). \tag{6}$$

The auxiliary term P^{aux} can be used for hooking additional observers or other corrective factors into the loop.

2) Frequency Control: Unobserved powers P^{uo} manifest themselves as deviations of the primary reserves from their f_0 setpoints:

$$0 = \Delta P^{\text{pri}} + P^{\text{uo}}, \tag{7}$$

with $\Delta P^{\text{pri}} = P^{\text{pri}} - P_0^{\text{pri}}$ as the primary deviations. Comparing (7) with (4) shows that $\Delta P^{\text{pri}} = -k\,(f - f_r)$ applies. Therefore, frequency can be indirectly observed over the primary resources' deviations. This allows for the calculation of the reference frequency

$$f_r^*(n+1) = f_0 + \frac{\Delta P^{\text{pri}}(n)}{k(n)}, \tag{8}$$

which mitigates steady-state errors for any given unobserved power.

3) Filtering: The balancing power $P^{\text{sec},*}(n+1)$ and reference frequency $f_r^*(n+1)$ need to be low-pass filtered before being applied to the system for various reasons: discrete-time sampling causes aliasing on measured quantities, which are also subject to measurement noise; improving stability margins by moving Eigenvalues away from the imaginary axis into the left side of the complex plane; and for smoothening the secondary response.

The filtered signals of (6) and (7) implemented in a discrete form are

$$P^{\text{sec}}(n+1) = P^{\text{sec}}(n) + \tfrac{T_{\text{c}}\omega_{\text{LP}}}{2\pi}\left(P^{\text{sec},*}(n+1) - P^{\text{sec}}(n)\right) \tag{9}$$

and

$$f_r(n+1) = f_r(n) + \tfrac{T_{\text{c}}\omega_{\text{LP}}}{2\pi}\left(f_r^*(n+1) - f_r(n)\right), \tag{10}$$

The filter cutoff must obey the control interval's Nyquist frequency but can otherwise be chosen as fast as desired:

$$\omega_{\text{LP}} < \tfrac{\pi}{T_{\text{c}}}. \tag{11}$$

Because the cutoff only depends on the control intervals, the DLFC can be considered tuning-free.

IV. Simulation

A MATLAB/Simulink simulation model was developed based on the model in Section III-A and Fig. 1. Primary and secondary resources exhibit ramp rate limitations P_{ramp}, and secondary control is subject to delay $T_{\text{delay}}^{\text{sec}}$. The considered control area has a total nominal generation capacity of $200\,\text{MW}$ and a droop of $5\,\%$. Load damping is set to $0.5\,\%$.

A. Scenarios

Two scenarios are considered, on which the AGC and DLFC are compared against each other in a single-area power system (see Fig. 1) modelled as a one-bus equivalent:

a) High-inertia Scenario J_{hi}: : This base case assumes predominantly synchronous machines in the total generation mix. Ramp limitations and secondary control delays are significant non-linearities that degrade the system response to transient events. The AGC is tuned for optimal performance in this scenario with a reference step size of $4\,\text{MW}$ (corresponding to $2\,\%$ of the nominal base power).

b) Low-inertia Scenario J_{lo}: : In this scenario we assume a high share of inverter-coupled resources able to react faster than synchronous machines. The resulting inertia is decreased, and higher ramp rates and lower control delays contribute to a much faster system response.

Table I lists the relevant system properties for both scenarios. Control intervals are $T_{\text{c}}^{\text{sec}} = 1\,\text{s}$, with a low-pass cutoff frequency (11) of $\omega_{\text{LP}} = \frac{1}{3}$.

A series of load events is applied on the system. Table II numbers the events in chronological order and describes the actions. We assume events 2 and 3 to be unobserved by the DLFC in order to highlight it's frequency control abilities under partial observability.

B. Results

This section features various performance evaluations of the AGC and DLFC on the high- and low-inertia scenarios described in Section IV.

TABLE I
SIMULATION SCENARIOS PROPERTIES.

Scenario	J_{hi}	J_{lo}
Inertia constant H (s) @ $S_{\text{base}} = 200\,\text{MVA}$	1.23	3.08
Ramp limit P_{ramp} ($\text{MW}\,\text{s}^{-1}$)	1	10
Ramp limit P_{ramp} ($\%\,\text{s}^{-1}$)	0.5	5.0
Secondary delay $T^{\text{sec}}_{\text{delay}}$ (s)	5	1
Secondary control interval $T^{\text{sec}}_{\text{c}}$ (s)	1	
Primary droop (%)	5	
Primary droop gain k^{c} ($\text{MW}\,\text{Hz}^{-1}$)	80	
Load damping (%)	0.5	
AGC proportional gain V^P (1)	0.07	
AGC integral time constant T^I (s)	16.67	
DLFC low-pass filter cutoff ω_{LP} ($\text{rad}\,\text{s}^{-1}$)	0.333	

TABLE II
SIMULATION EVENTS.

Event	Time (s)	Parameter	Parameter change	Note
1	10	ΔP^{obs} (MW)	$0 \to -4$	Reference event for AGC tuning in the high-inertia case
2	60	ΔP^{uo} (MW)	$0 \to 4$	Unobserved by DLFC
3	110	ΔP^{uo} (MW)	$4 \to 0$	Unobserved by DLFC
4	160	ΔP^{obs} (MW)	$-4 \to 3$	
5	210	ΔP^{obs} (MW)	$3 \to -6$	

1) Small-Signal Stability: A small-signal stability analysis is conducted in the following for assessing the controllers' responses to small disturbances. The system is linearized around the working point $100\,\text{MW}$ and $50\,\text{Hz}$ using MATLAB's Control Systems Toolbox. Ramp limitations are neglected in this study, but delays are incorporated. The resulting transfer function $G(s)$ is implicitly formulated in MATLAB due to the state delays (only input or output delays can be explicitly written down), and is therefore omitted in this work.

The closed-loop frequency response of the two controllers is shown in the Bode diagram in Fig. 2. The magnitude is normalized to the total droop capacity of the area. Both controllers behave similar for high-frequencies above $1/T^{\text{sec}}_{\text{c}}$, where the underlying inertial response of the system dominates. The range of $0.1\,\text{Hz}$ to $1\,\text{Hz}$ shows the response of the controllers to transient events like load steps. Here, the AGC exhibits a smoother response due to the inertia of the integrator, whereas the DLFC overshoots. Responsible for the overshooting are the two concurrent control actions, which translate to much faster settling times as can be seen for the lower frequencies. The DLFC has a $40\,\text{dB}$ falloff contrary to the AGC's $20\,\text{dB}$, hence steady-state deviations are mitigated faster. Contrary to the AGC, the DLFC also benefits from the faster system response in the low-inertia scenario. Both controllers run in both scenarios towards $-90°$ in the phase plot and therefore provide sufficient phase margin.

The pole-zero map in Fig. 3 shows that the Eigenvalues are in the left side of the complex plane, thus confirming

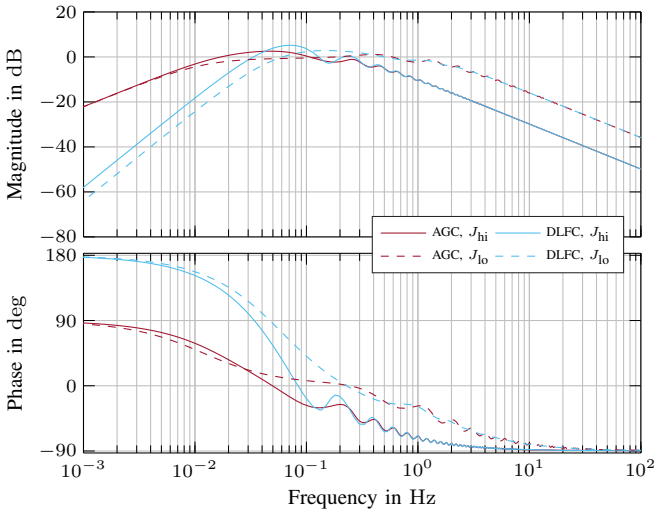

Fig. 2. Closed-loop frequency response of the AGC and DLFC for the high- and low-inertia scenarios. The magnitude is normalized to the total area's droop capacity.

stability in all considered cases. One pole is always present in the locus $(0, 0)$, which stems from the integral behavior of the swing equation (2). The response speed of the controllers in the different scenarios can be observed by the location of the poles, which move towards the left for the DLFC in the low-inertia case. However, the AGC's fastest pole remains unchanged as it does not adapt to the changing environment.

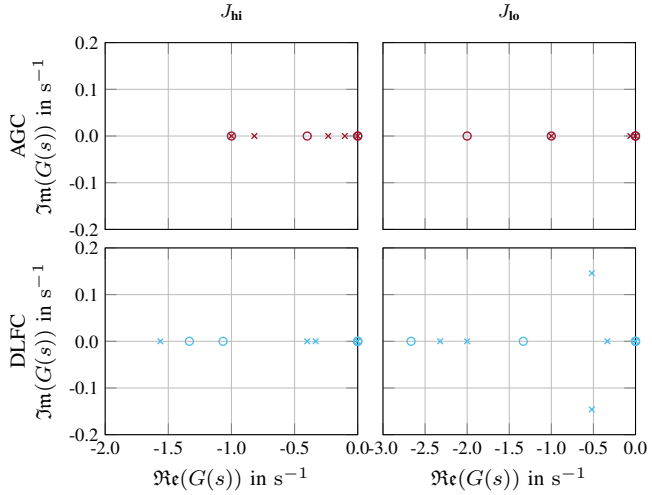

Fig. 3. Pole-zero map of the AGC and DLFC for the high- and low-inertia scenarios.

2) Transient Event Response: Ramp limitations and response delays of primary and secondary resources have a significant impact on balancing large load steps. Tuning of the AGC needs to consider these restrictions for achieving good response speed while maintaining stability. The controllers' performances are evaluated for the load steps in Table II.

Fig. 4 shows the system response for the high-inertia scenario with the AGC and DLFC, as well as using only

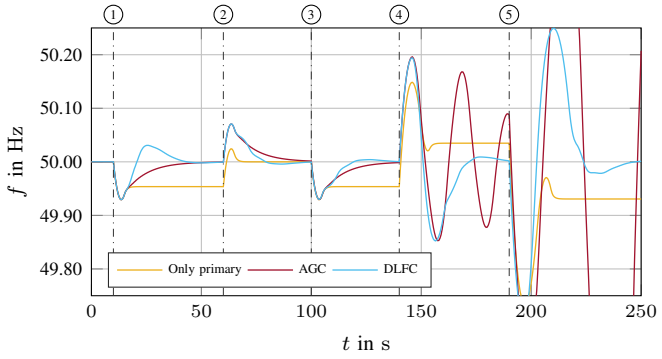

Fig. 4. System frequency response using primary control, AGC, and DLFC for the high-inertia scenario.

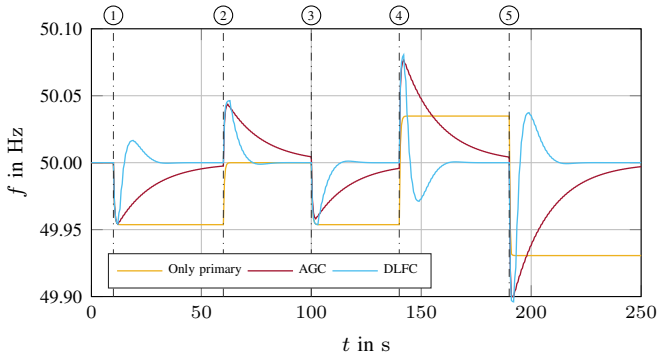

Fig. 5. System frequency response using primary control, AGC, and DLFC for the low-inertia scenario.

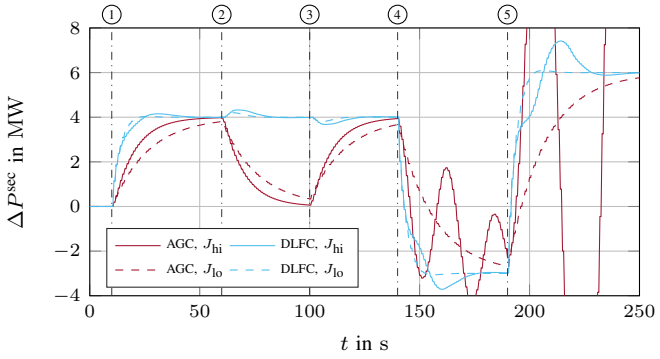

Fig. 6. Secondary power as activated by the AGC and DLFC for both scenarios.

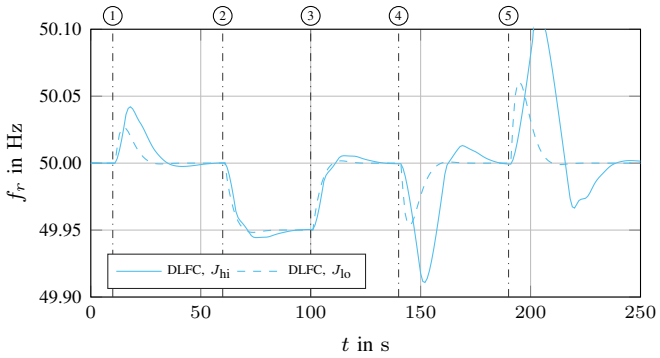

Fig. 7. Primary reference frequency determined by the DLFC in both scenarios.

primary control for comparison. Fig. 6 and Fig. 7 depict the corresponding secondary powers and primary reference frequencies, respectively. The effects of the limited ramp rates are illustrated in the primary control response, which exhibits increasing overshooting with larger step sizes before settling. Event 1 is the reference event against which the AGC was tuned; consequently, its response is fast and smooth. The DLFC, on the other hand, exhibits overshooting due to the two concurrent controller actions and settles slower compared to the AGC.

Overshooting is much less pronounced in case of events 2 and 3, which are assumed to be unobserved by the monitoring system. Hence, only the frequency control part of the DLFC is active, and primary devices cover the imbalance over the whole interval. Restoring primary reserves in this case requires an imbalance observer like the ACE, which can be hooked in via the P^{aux} term in (6).

The first major advantage of the proposed tuning-less approach becomes apparent in event 4, where the AGC's integrator winds up and causes oscillations, and in event 5, which finally destabilizes the system using AGC. The DLFC, on the other hand, remains stable as long as the primary resources are able to cover the imbalances. Its response changes accordingly in magnitude, but otherwise exhibits the same characteristic.

Examining the controllers' responses in the low-inertia case in Fig. 4 confirms the speed advantage of the DLFC as described in Section IV-B1. While none of the two secondary controls suffers from stability issues because of the higher ramp rates, the AGC does not benefit from the increased system response speed. On the contrary, the AGC's settling time worsens because its tuning is optimized for different non-linearities. The DLFC is in this case only limited by the secondary control intervals and the corresponding low-pass filter cutoff.

V. Conclusions & Outlook

This paper presented a novel tuning-less LFC approach called DLFC. It uses direct state observations from within the control area to determine secondary power setpoints and actively involves primary resources in frequency control. Numerical assessments confirm the DLFC's advantages over the AGC in terms of stability and speed for a wide range of system parameters. As the DLFC does not employ an integrator, its performance is limited only by the secondary control intervals and the reaction speed of primary and secondary resources. Entailed by the non-linear nature of power systems, the linear PI-controller of the AGC exhibits better performance than the DLFC just for specific working points it was tuned against. The DLFC's consideration of resource capabilities (power outputs, droop gain) in every control step via modern

monitoring and ICT infrastructure promotes the notion of "plug-and-play" power systems.

A practical implementation of this approach on a three-area laboratory power grid, incorporating networked control mechanisms with neighboring control areas as well as an analytical stability proof, can be found in the referenced manuscript [28]. Future works will further address: (i) An observer for powers unaccounted for by the monitoring system is necessary for freeing primary reserves, while maintaining the benefits of the DLFC; (ii) and dampening the DLFC's concurrent control actions to guarantee that the ACE does not overshoot as required by the ENTSO-E [29].

ACKNOWLEDGMENTS

The work in this paper has been supported by the European Commission under the FP7 project ELECTRA (grant no: 609687). Website: www.electrairp.eu.

REFERENCES

[1] B. I. J. Pérez-arriaga, "The Transmission of the Future," *IEEE Power Energy Mag.*, pp. 41–53, 2016.

[2] P. Tielens and D. Van Hertem, "The relevance of inertia in power systems," *Renew. Sustain. Energy Rev.*, vol. 55, pp. 999–1009, 2016.

[3] J. Von Appen, M. Braun, T. Stetz, K. Diwold, and D. Geibel, "Time in the sun: The challenge of high PV penetration in the German electric grid," *IEEE Power Energy Mag.*, vol. 11, no. 2, pp. 55–64, 2013.

[4] P. Kundur, *Power System Stability and Control*. McGraw-Hill,Inc, 1994.

[5] European Network of Transmission System Operators for Electricity (ENTSO-E), "Nordic Balancing Philosophy," tech. rep., June 2016.

[6] M. Farahani, S. Ganjefar, and M. Alizadeh, "PID controller adjustment using chaotic optimisation algorithm for multi-area load frequency control," *IET Control Theory Appl.*, vol. 6, no. 13, pp. 1984–1992, 2012.

[7] L. Dong, Y. Tang, H. He, and C. Sun, "An Event-Triggered Approach for Load Frequency Control With Supplementary ADP," *IEEE Trans. Power Syst.*, vol. 32, pp. 581–589, Jan 2017.

[8] H. A. Yousef, K. AL-Kharusi, M. H. Albadi, and N. Hosseinzadeh, "Load Frequency Control of a Multi-Area Power System: An Adaptive Fuzzy Logic Approach," *IEEE Trans. Power Syst.*, vol. 29, pp. 1822–1830, July 2014.

[9] D. Qian, S. Tong, H. Liu, and X. Liu, "Load frequency control by neural-network-based integral sliding mode for nonlinear power systems with wind turbines," *Neurocomp.*, vol. 173, Part 3, pp. 875–885, 2016.

[10] A. M. Ersdal, L. Imsland, and K. Uhlen, "Model Predictive Load-Frequency Control," *IEEE Trans. Power Sys.*, vol. 31, Jan 2016.

[11] X. Liu, Y. Zhang, and K. Y. Lee, "Robust distributed MPC for load frequency control of uncertain power systems," *Control Eng. Practice*, vol. 56, pp. 136–147, 2016.

[12] M. Ma, C. Zhang, X. Liu, and H. Chen, "Distributed Model Predictive Load Frequency Control of Multi-Area Power System after Deregulation," *IEEE Trans. Ind. Electron.*, vol. 4, no. 1, pp. 1–1, 2016.

[13] Y. Zhang, X. Liu, and B. Qu, "Distributed model predictive load frequency control of multi-area power system with DFIGs," *IEEE/CAA J. Automatica Sinica*, vol. 4, pp. 125–135, Jan 2017.

[14] A. Pappachen and A. Peer Fathima, "Critical research areas on load frequency control issues in a deregulated power system: A state-of-the-art-of-review," *Renewable Sustain. Energy Reviews*, vol. 72, no. January 2016, pp. 163–177, 2017.

[15] S. C. Tong, Y. M. Li, and H. G. Zhang, "Adaptive Neural Network Decentralized Backstepping Output-Feedback Control for Nonlinear Large-Scale Systems With Time Delays," *IEEE Trans. Neural Netw.*, vol. 22, pp. 1073–1086, July 2011.

[16] G. Giannakis, V. Kekatos, and N. Gatsis, "Monitoring and optimization for power grids: A signal processing perspective," *IEEE Signal Process. Mag.*, no. Aug. 2013, pp. 107 – 128, 2013.

[17] A. Prostejovsky, O. Gehrke, M. Marinelli, and M. Uslar, "Reduction of Topological Connectivity Information in Electric Power Grids," in *Univ. Power Eng. Conf. (UPEC), 2016 Proc. 51st Inter.*, pp. 1–6, Sept. 2016.

[18] Agency for the Cooperation of Energy Regulators (ACER), "Energy Regulation: A Bridge to 2025," Sept. 2014. [Online]. Available: http://www.acer.europa.eu. Accessed on May 11, 2017.

[19] V. Gungor, D. Sahin, T. Kocak, S. Ergut, C. Buccella, C. Cecati, and G. Hancke, "A Survey on Smart Grid Potential Applications and Communication Requirements," *IEEE Trans. Ind. Informat.*, vol. 9, pp. 28–42, Feb 2013.

[20] Union of the Electricity Industry - EURELECTRIC, "EURELECTRIC's vision about the role of Distribution System Operators (DSOs) - A EURELECTRIC paper," tech. rep., February 2016. [Online]. Available: http://www.eurelectric.org. Accessed on May 18, 2017.

[21] European Commission, "Cost-benefit analyses & state of play of smart metering deployment in the EU-27 ," tech. rep., June 2014. http://eur-lex.europa.eu [Accessed: 01-05-2017].

[22] M. Rezkalla, K. Heussen, M. Marinelli, J. Hu, and H. W. Bindner, "Identification of requirements for distribution management systems in the smart grid context," in *Power Eng. Conf. (UPEC), 2015 50th Int. Universities*, pp. 1–6, Sept 2015.

[23] CEN-CENELEC-ETSI Smart Grid Coordination Group, "Smart Grid Reference Architecture," no. November, pp. 1–46, 2012.

[24] European Distribution Systems Operators' Association for Smart Grids, "TSO – DSO Management Report," july 2016. http://www.edsoforsmartgrids.eu [Accessed: 19-03-2017].

[25] Office of Energy Policy and Systems Analysis, "Standards and Interoperability in Electric Distribution Systems," October 2016. [Online]. https://energy.gov. Accessed on May 18, 2017.

[26] R. D'hulst, J. M. Fernández, E. Rikos, *et al.*, "Voltage and frequency control for future power systems: the ELECTRA IRP proposal," in *2015 Int. Symp. Smart Electric Distribution Systems and Technologies (EDST)*, pp. 245–250, Sept 2015.

[27] C. Caerts *et al.*, "Specification of Smart Grids high level functional architecture for frequency and voltage control," *ELECTRA Deliverable D3.1. WP3 Scenarios and case studies for future power system*, Apr. 2015. [Online]. http://www.electrairp.eu.

[28] A. M. Prostejovsky, M. Marinelli, M. Rezkalla, M. H. Syed, and E. Guillo-Sansano, "Tuning-less Load Frequency Control Through Active Engagement of Distributed Resources," *IEEE Transactions on Power Systems*, 2017. Under review. Manuscript submitted 2017-03-20.

[29] European Network of Transmission System Operators for Electricity (ENTSO-E), "P1 – Policy 1: Load-Frequency Control and Performance," tech. rep. [Online]. Available: http://www.entsoe.eu. Accessed on May 18, 2017.